Received: 10 June 2021 | Revised: 30 August 2021 | Accepted: 3 October 2021

DOI: 10.1111/cas.15159

ORIGINAL ARTICLE

Cancer Science WILEY

Non-metabolic function of MTHFD2 activates CDK2 in bladder cancer

Xi Liu | Shuangjie Liu | Chiyuan Piao | Zhe Zhang | Xiaotong Zhang | Yuanjun Jiang | Chuize Kong

Department of Urology, The First Hospital of China Medical University, Shenyang, China

Correspondence
Yuanjun Jiang and Chuize Kong, Department of Urology, The First Hospital of China Medical University, Shenyang 110001, China.
Emails: 13804064945@163.com (YJ); kongchuize_cmu@sina.cn (CK)

Funding information
Liaoning Clinical Medical Research Center, (Grant/Award Number: 'Grant No. [2020]44') Shenyang Clinical Medical Research Center, (Grant/Award Number: 'Grant No. 20-204-4-42') Shenyang Plan Project of Science and Technology, (Grant/Award Number: 'Grant No. F19-112-4-098') National Key R&D Plan Key Research Projects of Precision Medicine, (Grant/Award Number: '2017YFC0908000')

Abstract

Bladder cancer is a common tumor with a high recurrence rate and high fatality rate, and its mechanism of occurrence and development remains unclear. Many proteins and metabolites reprogram at different stages of tumor development to support tumor cell growth. The moonlighting effect happens when a protein performs multiple functions simultaneously in a cell. In this study, we identified a metabolic protein, MTHFD2, which participates in the cell cycle by binding to CDK2 in bladder cancer. MTHFD2 has been shown to affect bladder cancer cell growth, which is independent of its metabolic function. We found that MTHFD2 was involved in cell cycle regulation and could encourage cell cycle progression by activating CDK2 and sequentially affecting E2F1 activation. In addition, moonlighting MTHFD2 might be regulated by the dynamics of the mitochondria. In conclusion, MTHFD2 localizes in the nucleus to perform a distinct function of catalyzing metabolic reactions. Moreover, the nuclear MTHFD2 activates CDK2 and promotes bladder cancer cell growth by modulating the cell cycle.

KEYWORDS
bladder cancer, CDK2, cell cycle, moonlighting protein, MTHFD2

1 | INTRODUCTION

Bladder cancer (BC), the most common type of cancer of the urinary system worldwide, can be divided into 2 groups: non-muscle-invasive bladder cancer (NMIBC) and muscle-invasive bladder cancer (MIBC). NMIBC is usually benign, but it may recur or progress to an MIBC. MIBC is frequently associated with poor prognosis and has limited effective therapies.[1] Therefore, understanding the mechanism of bladder cancer progression is important in the development of related therapies.

MTHFD2 is a metabolic gene that mainly participates in one-carbon metabolism. The enzymatic activity of MTHFD2 transfers 5,10-methylene-tetrahydrofolate (CH2-THF) and $NAD(P)^+$ to 10-formyl-THF (CHO-THF) and NAD(P)H.[2,3] The products of the one-carbon cycle participate in many life processes, such as energy supplementation, nuclear acid synthesis, and amino acid synthesis.[4,5] MTHFD2 is highly expressed during embryo development and its expression decreases as one ages..[6] In various types of solid tumors, it is re-expressed and promotes tumor progression.[7-9] However, its role in bladder cancer development remains unclear.

Moonlighting proteins (MPs) are a special type of protein with multiple independent functions. Moreover, they have been found in many metabolic proteins due to pathological changes.[10] In addition to reprogramming metabolites, MPs are also recognized to perform

the noncanonical or non-metabolic functions of metabolic enzymes as they directly modulate cell signaling and epigenetic pathways.[11] It has been reported that MTHFD2 can participate in nuclear DNA synthesis in different cells.[12,13] In addition, a similar protein in the one-carbon cycle, MTHFD1, has been found to bind to BRD4 and regulate epigenetic processes.

The cell cycle is regulated by several exact signaling pathways that go through different phases independently.[14] The threshold of E2F1 and Myc expression is an important checkpoint for cells entering the S phase. The activation of CDK2 usually starts in the late G1 phase, increases rapidly in the S phase, and ends with mitosis.[15] In the G1 phase, CDK2 releases E2F1 from retinoblastoma (Rb) after phosphorylation by CDK4 and CDK6, while CDK2 activates E2F1 by co-working with cyclin A in the S phase.[16]

MTHFD2 is mainly distributed in the mitochondria based on structure prediction. Therefore, its participation in biological activities in other organelles remains unclear. The coordinated cycles of fission and fusion are referred to as mitochondrial dynamics. These are essential for maintaining mitochondrial quality. Mitochondrial fusion provides placement for metabolic reactions, material synthesis, and content exchange, while fission is vital for mitochondrial autophagy and updates.[17,18] In the cell cycle, mitochondria fuse into a tubular formation at the G1-S phase and induce cell cycle-related protein changes via an unknown mechanism.[19] Therefore, we hypothesized the presence of some essential communication between the mitochondrial dynamics and the cell cycle.

Here, we identified that MTHFD2 activated CDK2 in bladder cancer cells, functioning as a moonlighting protein. Precipitation was independent of the metabolic function of MTHFD2 and could promote tumor cell growth. Furthermore, verification of the effectors of CDK2 activation, namely E2F1, indicated that the moonlighting function of MTHFD2 regulates the cell cycle in the G1-S phase through the CDK2-Rb axis. Additionally, we found that nuclear-translocated MTHFD2 might be associated with mitochondrial dynamics, which would increase its nucleus-localized function. This study elucidates a novel mechanism of MTHFD2 in cells and provides an optional target for clinical therapeutics.

2 | MATERIALS AND METHODS

2.1 | Patients and cells

Forty tissue samples were surgically collected from participants who were treated for bladder cancer at the First Affiliated Hospital of China Medical University. All participants provided informed consent. The study was designed and all procedures were carried out in accordance with the guidelines of the Institutional Ethics Committee of China Medical University (Approval No. [2021]121). The patient characteristics regarding the samples are provided in Table S1. HEK-293T and bladder tumor cell lines, UMUC3 and T24, were purchased from the Cell Bank of the Chinese Academy of Sciences and cultured in high glucose DMEM medium (Gibco, Thermo Fisher Scientific, Inc) supplemented with 10% FBS (Gibco) at 37°C in 5% CO_2.

2.2 | Reagents

Two μmol/L CVT-313 (Selleck), an effective ATP-competitive selective CDK2 inhibitor, was incubated for 12 h and used for UMUC3 and T24. Mdivi-1 (Selleck), a mitochondrial division inhibitor 1, is a selective transmembrane inhibitor of mitochondrial division that inhibits DRP1 and dynamin I (Dnm1). Five μmol/L Mdivi-1 was incubated with the cell cultures for 24 h. Mito-Tracker Red (Beyotime) was used at a concentration of 200 μmol/L for 15 min to stain the mitochondria. Nocodazole (Selleck) was applied at a dosage of 100 nmol/L for 12 h to induce the synchronization of cells. Then, the synchronized cells were released in a fresh medium.

2.3 | NAD/NADH assay

The NAD/NADH assay was performed using the NAD/NADH-Glo™ Assay kit (Promega). Cells were lysed using 1% DTAB and heated at 60°C to extract NADH. They were also treated with 0.4 N HCl before heating to extract NAD^+. The lysate was incubated with NAD/NADH-Glo™ Detection Reagent and measured using a fluorescence microplate reader (BioTek).

2.4 | Cell transfection

Cell transfection was performed using LipoFiter 3.0 (HANBIO Corporation) and the results were analyzed after 48 h. The siRNA sequences are listed in Table S2. A stable expression cell line was constructed using a lentivirus packing plasmid system, and transfected cells were treated with puromycin (5 μg/mL) to reveal the positive cells. The plasmids used are listed in Table S2. Transiently transfected cells were used 48 h after transfection.

2.5 | Sphere formation assay

Here, 1000 cells per well were plated in ultra-low attachment 6-well flasks (Corning) for 3D culture. Serum-free medium (DMEM/F12; 1:1 mixture) supplemented with βFGF (20 ng/mL), B27 (1:50), and EGF (20 ng/mL; Invitrogen) was used for cell growth. The spheres were imaged after 10 d.

2.6 | 5-Ethynyl-2'-deoxyuridine (EdU) assay

5-Ethynyl-2'-deoxyuridine (50 μmol/L; RiboBio) was added, and the cells were cultured for an additional 2 h. The cells were then stained with the Cell-Light™ EdU Apollo®488 In Vitro Flow Cytometry Kit

(RiboBio) according to the manufacturer's protocol. The cells were photographed using a fluorescence microscope (Olympus) and analyzed using ImageJ software.

2.7 | Real-time cell analysis

Cells were seeded in cell culture E-plates at a density of 3000 cells per well and cultured at 37°C and under 5% CO_2. Average cell growth curves were automatically recorded and normalized at 6 h after seeding in real-time using the xCELLigence System (Roche Applied Science). The cell index was followed for 72 h.

2.8 | Western blotting

Total cell lysates were extracted using radioimmunoprecipitation assay buffer containing protease, phosphatase, and deacetylase inhibitors. Nuclear lysates were extracted using nuclear lysis buffers (Cell Signaling Technology) containing protease, phosphatase, and deacetylase inhibitors, as described in the manuscript. Proteins were separated using 10% SDS-PAGE and transferred onto polyvinylidene fluoride membranes. The membranes were blocked at room temperature for 2 h, incubated with the primary antibody at 4°C overnight, and incubated for 1 h with the appropriate secondary antibody. The antibodies used are listed in Table S2.

2.9 | Flow cytometry

Nuclear protein quantification was carried out by flow cytometry. First, permeabilization was performed to dissolve the cytoplasmic content using a cytoskeletal buffer containing 0.5% Triton X-100, 0.5% NP-40, and protease inhibitors. Cells were then fixed with 4% paraformaldehyde and blocked with 1% BSA. Cells were incubated with the diluted antibody overnight at 4°C, and with the fluorescent secondary antibody for 1 h at 37°C. The isotype control was incubated only with the secondary antibody. Cells were then measured using flow cytometry (BD Biosciences) using a FACScan instrument (BD Biosciences) and analyzed using FlowJo (BD Biosciences).

2.10 | Immunofluorescence (IF)

Cells were fixed with 4% paraformaldehyde, permeabilized with 2% Triton X-100, and blocked with 1% BSA. Primary antibodies were incubated with the cells overnight at 4°C and the fluorescent secondary antibody was incubated for 1 h at 37°C. For multicolor immunostaining, simultaneous incubation was performed with antibodies from different species, while sequential incubation was performed with antibodies from the same species. DAPI (1 μg/mL) staining was performed, and images were photographed using a fluorescence microscope (Olympus). Additionally, for nuclear immunostaining, a cytoplasm-dissolving step was also performed before fixation, and 100% methanol at −20°C was used for fixation.

2.11 | Co-Immunoprecipitation

Total cell and nuclear lysates were extracted as described above, and the lysates were incubated with antibodies at 4°C overnight using a rotator. Magnetic beads were pre-cleaned and co-incubated with the lysates and antibodies for another 4 h. The precipitated proteins were extracted and separated from the magnetic beads by heating with a loading buffer containing SDS.

2.12 | Chromatin immunoprecipitation

Cells were analyzed using the SimpleChIP® Enzymatic Chromatin IP Kit (Cell Signaling Technology). Cells were cross-linked with formaldehyde, and chromatin fragmentation in the nucleus was induced using a micrococcal nuclease and sonication. Chromatin was incubated with antibodies at 4°C overnight with rotation and co-incubated with magnetic beads for another 4 h. Chromatin was eluted from the protein using a thermomixer and purified using spin columns. The quantification of DNA was finally carried out using RT-qPCR. Several promoter primers of MTHFD2 were designed at high acetylation and tri-methylation levels at the promoter and the first exon region from the UCSC browser. The efficiency of MYC promoter primers from previous studies was evaluated and the most efficient primers are listed inTable S2.[20]

2.13 | Reverse transcription-quantitative polymerase chain reaction

Total RNA was extracted from tissue samples or cells using TRIzol reagent and then used for cDNA synthesis with the PrimeScript RT Master Mix kit (Takara Bio). Quantitative RT-PCR analysis was performed using the SYBR Premix Ex Taq kit (Takara Bio). The primer sequences are listed in Table S2.

2.14 | In vivo model for tumor growth

Ten female 4-wk-old BALB/c nude mice were obtained from (Vital River Laboratory Animal Technology Co) for xenograft experiments. All experiments were performed in the animal center at China Medical University and were conducted in accordance with the institutional guidelines and approved by the Animal Care and Use Committee (IACUC Issue No. 2020005). The mice were randomized into 2 groups of 5 each and 1.5×10^7 cells were subcutaneously injected. All mice were housed, and tumors were harvested after 5 wk of observation.

2.15 | Mass spectrometry

A gel with proteins precipitated with MTHFD2 was prepared. The proteins were identified using mass spectrometry and commissioned by Novogene Corporation. In brief, liquid chromatography-MS/MS analysis was performed using a Q Exactive HF-X mass spectrometer (Thermo Fisher Scientific), with Nanospray Flex™ serving as the ion source, and the identification of proteins was carried out using Proteome Discoverer 2.2 (PD 2.2, Thermo Fisher Scientific).

2.16 | Bioinformatic analysis

Eighteen datasets were downloaded from The Cancer Genome Atlas Program (TCGA), Gene Expression Omnibus (GEO), and the European Bioinformatics Institute (EMBL) databases. Detailed information is provided in Table S3. The WGCNA package in R was used for analysis,[21] and the expression of MTHFD2 in datasets was extracted for further analysis. The ClusterProfiler package in R was used for KEGG and GSEA analyses.[22] The Seurat package in R was used for scRNA analyses. The Cytohubba package in Cytoscape software (v3.6.1) was used for protein interaction score evaluation.[23]

2.17 | Statistical analysis

Experimental data are presented as the mean ± SD of at least 3 independent experiments. Differences between the groups were analyzed using Student *t* test or one-way ANOVA. Differences between the groups in clinical data were evaluated using the Kruskal-Wallis test, Mann-Whitney test, or Wilcoxon test. Survival status was analyzed using Kaplan-Meier and log-rank methods.

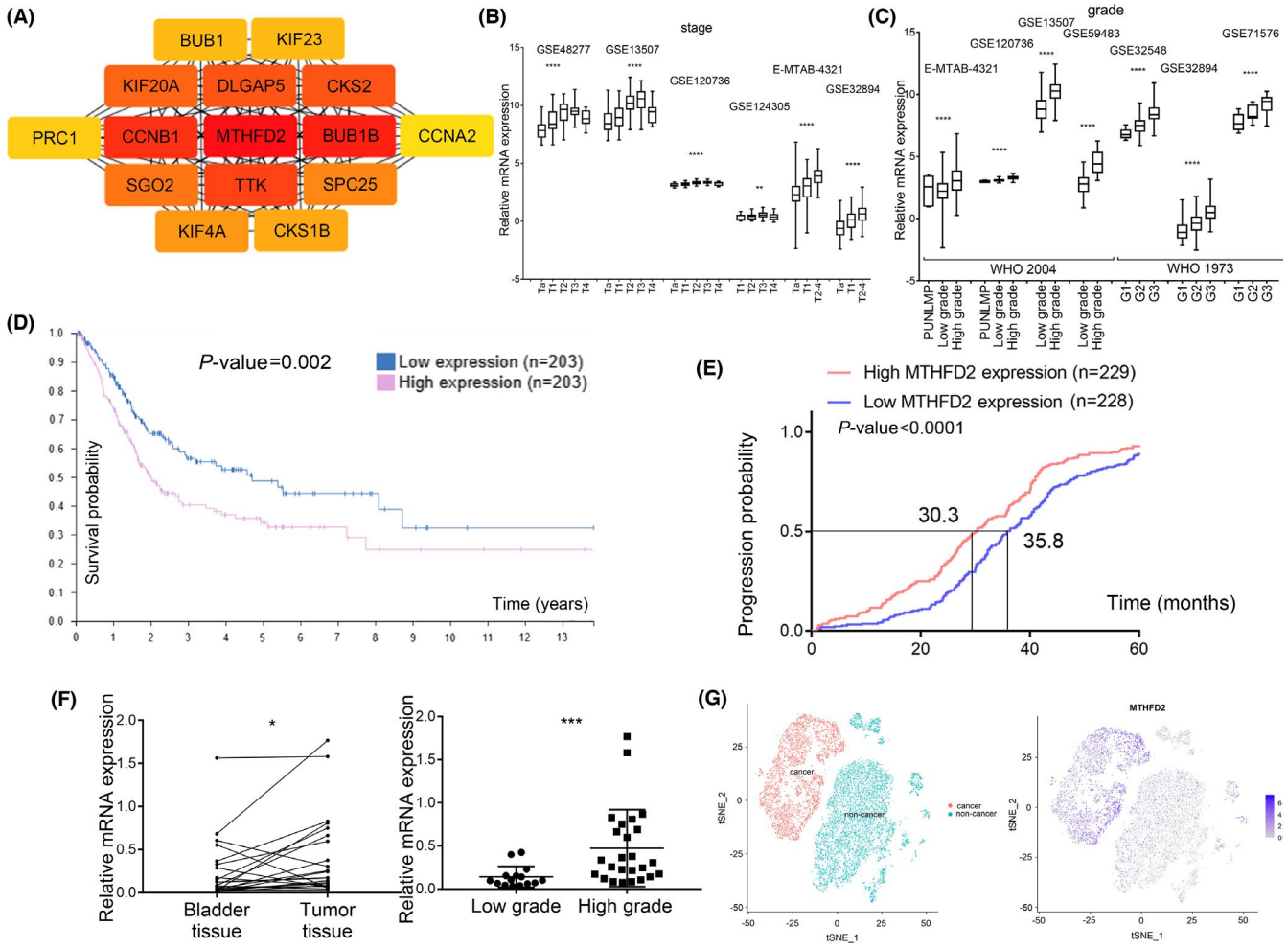

FIGURE 1 MTHFD2 corresponded with a worse prognosis in bladder cancer. A, A protein interaction network for the module of WGCNA analysis associated with bladder cancer grade and cell cycle using the GSE32894 dataset. B, Expression of MTHFD2 about tumor stage from different bladder cancer datasets. C, Expression of MTHFD2 about tumor grade from different bladder cancer datasets. D, Survival probability grouped by MTHFD2 of MIBC from TCGA dataset. E, Progression probability grouped by MTHFD2 of NMIBC from the Uromol dataset. F, Collected bladder cancer tissue showed MTHFD2 is highly expressed in high-grade tumor sample. G, MTHFD2 expressed specifically in cancer cells clustered from integrated single-cell RNA sequence data

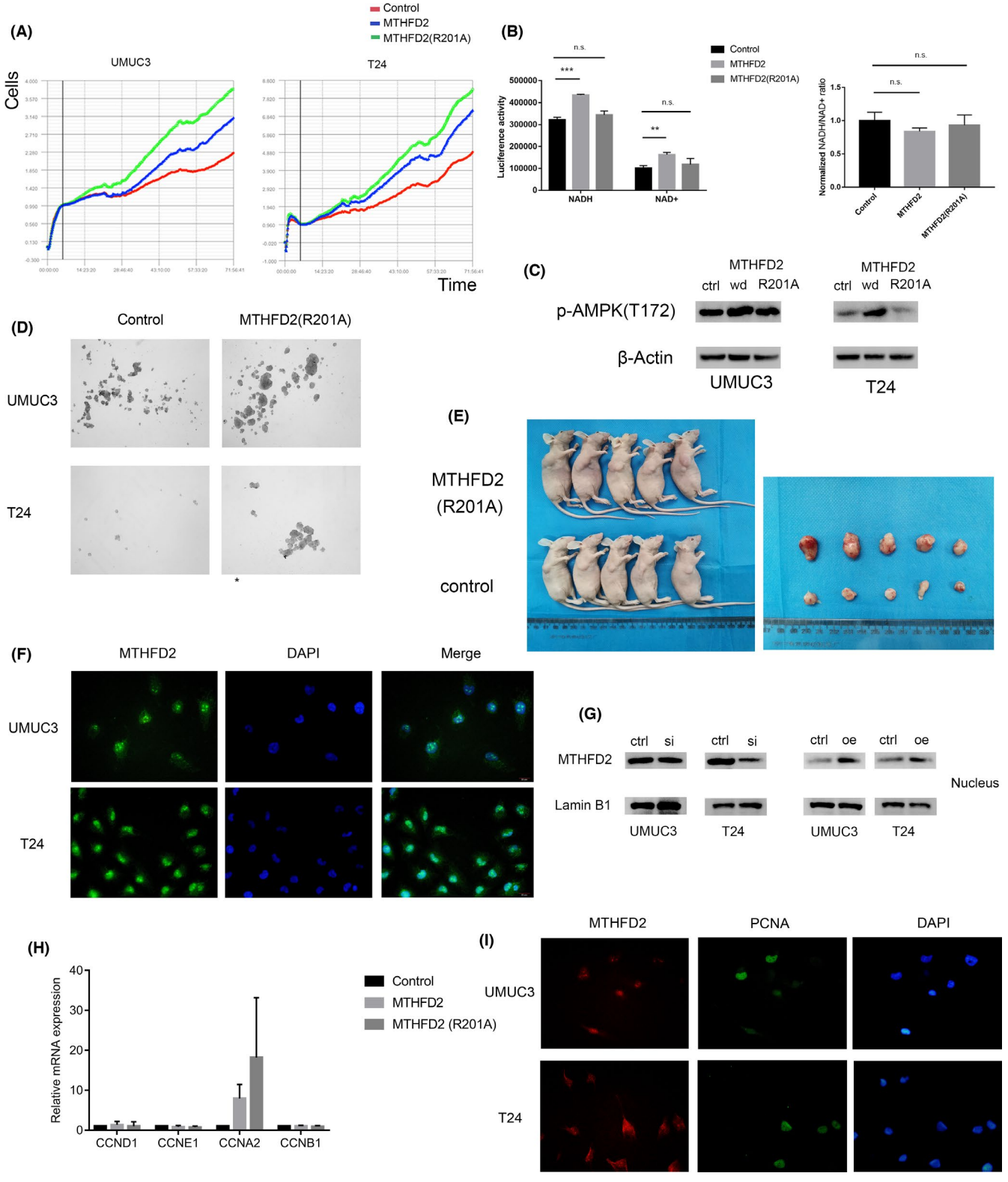

FIGURE 2 MTHFD2 promoted proliferation with the non-enzyme function in bladder cancer cells. A, Normalized average cell growth curve recorded by RTCA of wild-type MTHFD2 or mutated MTHFD2 cells. B, Enzyme function of MTHFD2 and mutated MTHFD2 measured by the content of NAD^+ or NADH and NAD^+/NADH ratio. C, Downstream protein signal change in MTHFD2 or mutated MTHFD2 cells. D, Tumor sphere 3D-culture performed by mutated MTHFD2 bladder cancer cells. E, In vivo model for mutated MTHFD2. F, Localization of MTHFD2 in bladder cancer cells by IF. G, Nuclear MTHFD2 change after MTHFD2 knockdown or overexpression. H, Different cyclins expression in wild-type MTHFD2 or mutated MTHFD2 UMUC3 bladder cancer cells. I, Distinguishing cell phase about nuclear MTHFD2 expression through identifying S-phase cell co-localized by PCNA

Statistical analysis was performed using Prism software (version 7.0; GraphPad). Statistical significance was set at $P < .05$ (*$P < .05$; **$P < .01$; and ***$P < .001$).

3 | RESULTS

3.1 | MTHFD2 corresponds with a worse prognosis in bladder cancer

By linking the clinical message to gene expression utilized by WGCNA, we identified a core gene, MTHFD2, relative to the stage and grade of bladder cancer, which is the most correlated to the prognosis (Figure S1A,B). For most genes in this module, their functions were enriched in the process of cell cycle or DNA replication (Figure 1A). MTHFD2, a mitochondrial serine metabolic enzyme that is generally removed from these genes and involved in this process, might have promised itself an unclassical behavior in determining the destiny of tumor cells.

A comparison of various public cohorts showed that MTHFD2 was more likely to be expressed in high-grade or malignant bladder tumors (Figure 1B,C). The survival or progression rate in either MIBC or NMIBC was significantly worse in the MTHFD2 high group (Figure 1D,E). Furthermore, verification with local samples confirmed that MTHFD2 was expressed in high-grade tumors and that MTHFD2 expression in tumor tissue was consistent with the public data (Figure 1F). At the single-cell level, MTHFD2 was significantly expressed in cancer cells (Figures 1G and S1C,D). Evidence from these clinical data showed that MTHFD2 is involved in bladder cancer development. Furthermore, tissue staining images illustrated the distribution of MTHFD2 in bladder cancer (Figure S2C,D).

3.2 | MTHFD2 promotes proliferation with the non-enzyme function in bladder cancer cells

By manipulating the expression of MTHFD2, a change occurred in the proliferation of bladder cancer cells. When MTHFD2 was knocked down, cells proliferated at a slower rate. Conversely, cells grew faster in the artificially expressed MTHFD2 group (Figures 2A and S2A). MTHFD2 is involved in the one-carbon cycle, providing material for nucleotide and amino acid synthesis. To further evaluate whether MTHFD2 promotes cell proliferation due to its metabolic function, we constructed a subtype of MTHFD2 mutated R201A that lacks the enzyme function. The loss of its enzyme activity was tested by its ability to produce NADH compared with the wild-type (Figure 2B). In addition, the metabolic process induced by MTHFD2 could activate AMPK,[2] while we found that the enzyme-mutated MTHFD2 abolished phosphorylated AMPK (Figure 2C). Surprisingly, we found a similar result between the wild-type and enzyme deletion type in the RTCA proliferation assay and sphere formation assay, indicating that MTHFD2 utilized an extra way to engage in cell growth (Figure 2A,D), and this was further verified in vivo (Figures 2E and S2D).

Fluorescence localization revealed that MTHFD2 was expressed in both the mitochondria and nuclei, and this indicated that MTHFD2 would have an additional function in the nucleus (Figure 2F). When manipulating MTHFD2, we found a significant change in the amount of nuclear MTHFD2 (Figure 2G). As mentioned above, MTHFD2 was correlated with the cell cycle pathway in the bladder cancer cohort. We found that MTHFD2 was highly correlated with CCNA2 and CCNB1 in bladder tissue (Figure S2B). In addition, it was found that artificially expressed non-enzyme activity of MTHFD2 could increase the expression of CCNA2 (Figure 2H). Further staining of cell nuclei showed that MTHFD2 was expressed throughout the cell cycle compared with the S-phase protein PCNA. This means that MTHFD2 was active not only at the S-phase but throughout the cell cycle (Figure 2I). Therefore, we considered that MTHFD2 expression in the nucleus would be involved in cell cycle control.

3.3 | MTHFD2 activates CDK2

To explore how MTHFD2 functions in the nucleus, we introduced a mass spectrum to show partner proteins co-working with MTHFD2 in bladder cancer cells. The annotation of subcellular localization showed that MTHFD2 was distributed in mitochondria and nuclei (Table S4). In the nucleus, these proteins were enriched in DNA replication. Moreover, further verification that MTHFD2 co-localized and co-precipitated with CDK2 in bladder cancer tissue and cells (Figures 3A,B,E and S3A-C). Unlike cyclins, which require CDK2 to be phosphorylated before binding, the precipitation between MTHFD2 and CDK2 was unrelated to its phosphorylation status or ATP binding region. This also indicates that MTHFD2 was not a phosphorylated target of CDK2 (Figure 3C).

A typical function for CDK2 involves the phosphorylation of the C-terminus of Rb followed by CDK4/6 and delivering the E2F family to initiate the cell cycle; therefore, we tested several phosphorylation

FIGURE 3 MTHFD2 activated CDK2. A, Co-localization of MTHFD2 and CDK2 in bladder cancer cells. B, Co-IP of CDK2 and Rb by MTHFD2 in UMUC3 bladder cancer cells. C, Co-IP of wild-type, mutated ATP binding region and phosphorylation site mutated CDK2 by MTHFD2 in UMUC3 bladder cancer cells. D, Co-IP of CDK2 and MTHFD2 by different Rb phosphorylation sites in UMUC3 bladder cancer cells. E, Co-IP of wild-type and mutated MTHFD2 by CDK2 in UMUC3 bladder cancer cells. F, Western blot of Rb phosphorylation sites regulated by CDK2 showed a reverse effect after applying CDK2 inhibitor, CVT-313, on mutated MTHFD2 in UMUC3 bladder cancer cells. G, ChIP of Myc promotor showing the binding of E2F1 on chromatin affected by non-metabolic mutated MTHFD2 or MTHFD2 knockdown in UMUC3 bladder cancer cells. H, Co-IP of acetylated lysine to identify E2F1 acetylation of wild-type MTHFD2 or mutated MTHFD2 UMUC3 bladder cancer cells. I, Identification of E2F1 acetylation of MTHFD2 knockdown UMUC3 bladder cancer cells

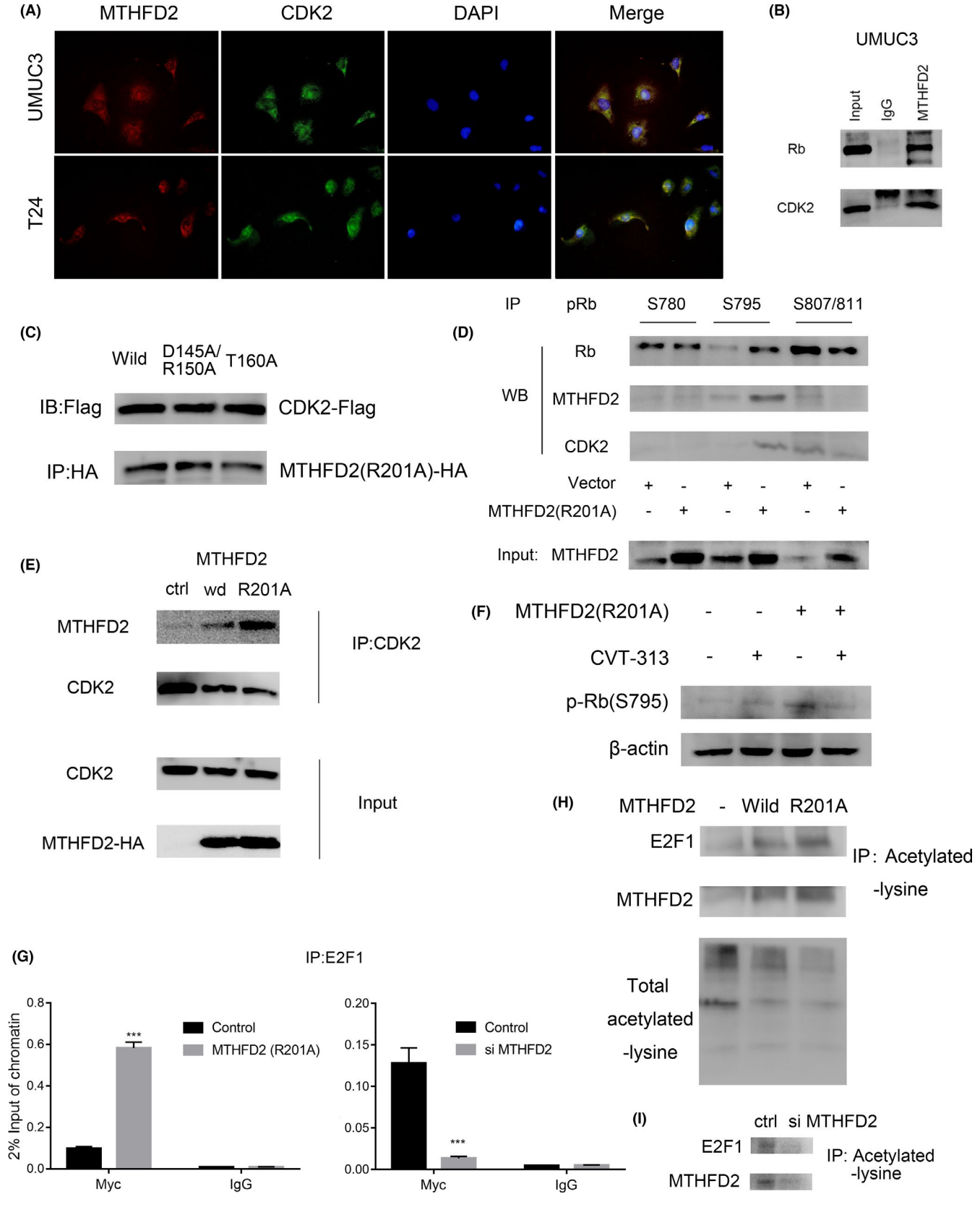

sites of Rb when overexpressing MTHFD2. As a result, Rb S795 was significantly activated compared with other phosphorylation sites (Figure 3D). Furthermore, the activity of CDK2, which was inhibited by CVT-313, reversed the phosphorylation of Rb S795 triggered by the MTHFD2 expression. This indicates that the activation of Rb by MTHFD2 was mediated by CDK2 (Figures 3F and S3D).

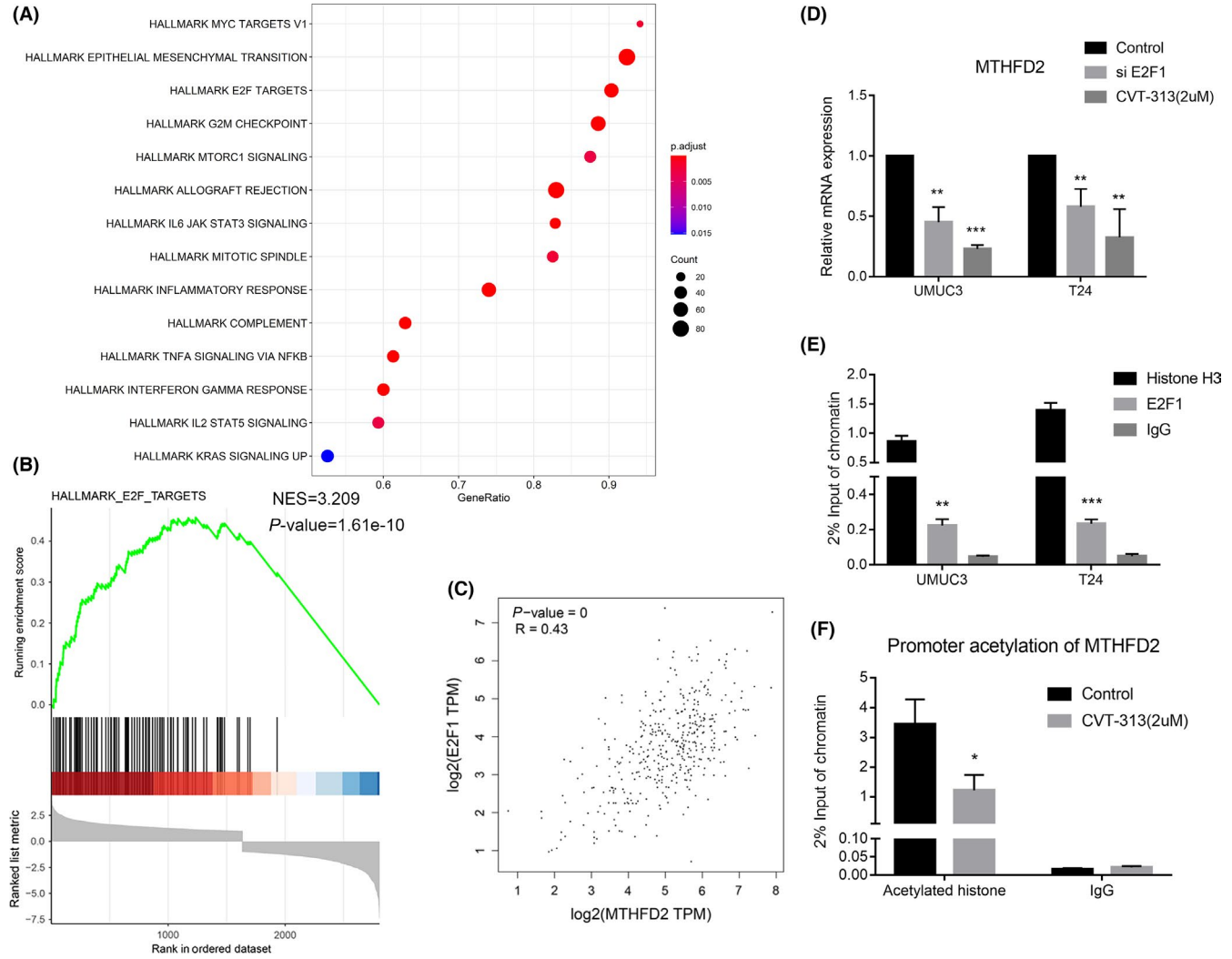

FIGURE 4 MTHFD2 transcriptional regulated by E2F1. A, Msigdb Hallmark Pathway Enrichment of differently expressed genes grouped by MTHFD2 expression from TCGA. B, GSEA analysis showed the gene involved in the E2F target pathway was correlated with MTHFD2 expression. C, A Pearson correlation analysis between the expression of E2F1 and MTHFD2 from TCGA dataset. D, Change of MTHFD2 expression after disturbing E2F1 expression or CDK2 activity in bladder cancer cells. E, ChIP assay showed that E2F1 would bind with the promoter of MTHFD2 in bladder cancer cells. F, ChIP assay showed that the acetylation level of MTHFD2 promoter region was inhibited by CDK2 inhibitor in UMUC3 bladder cancer cells

E2F1 is a transcription factor that acts as the downstream effector of CDK2 activation participating in the G1 and S phase cell cycle; therefore, we analyzed whether the activity of E2F1 would be altered by MTHFD2 stimulation. The acetylation of E2F1 was associated with E2F1 activation. We found that the manipulation of MTHFD2 altered the binding of E2F1 to the DNA promoter region (Figure 3G).[24] Furthermore, although E2F1 expression did not significantly change in MTHFD2-manipulated cells, the level of E2F1 acetylation altered in MTHFD2-manipulated cells (Figure 3H,I). These results indicated that MTHFD2 in bladder cancer cells could activate CDK2, which phosphorylates Rb and consequently increases E2F1 transcription activity independent of its metabolic function.

3.4 | MTHFD2 transcription regulated by E2F1

In bioinformatics analysis from the TCGA dataset, we found that many cell cycle pathways were associated with MTHFD2 expression levels (Figure 4A). Among them, the E2F target pathway was one of the most enriched pathways, indicating that MTHFD2 might be involved in the cell cycle phase and be transcriptionally regulated (Figure 4B). In addition, a significant correlation was observed between E2F1 and MTHFD2 in the dataset (Figure 4C). A decrease in the expression of MTHFD2 was found when E2F1 was knocked down or CDK2 activity was inhibited (Figure 4D). Moreover, we identified E2F1 binding to the promoter region of MTHFD2. Moreover, the blockage of CDK2 activity reduced E2F1 binding and histone

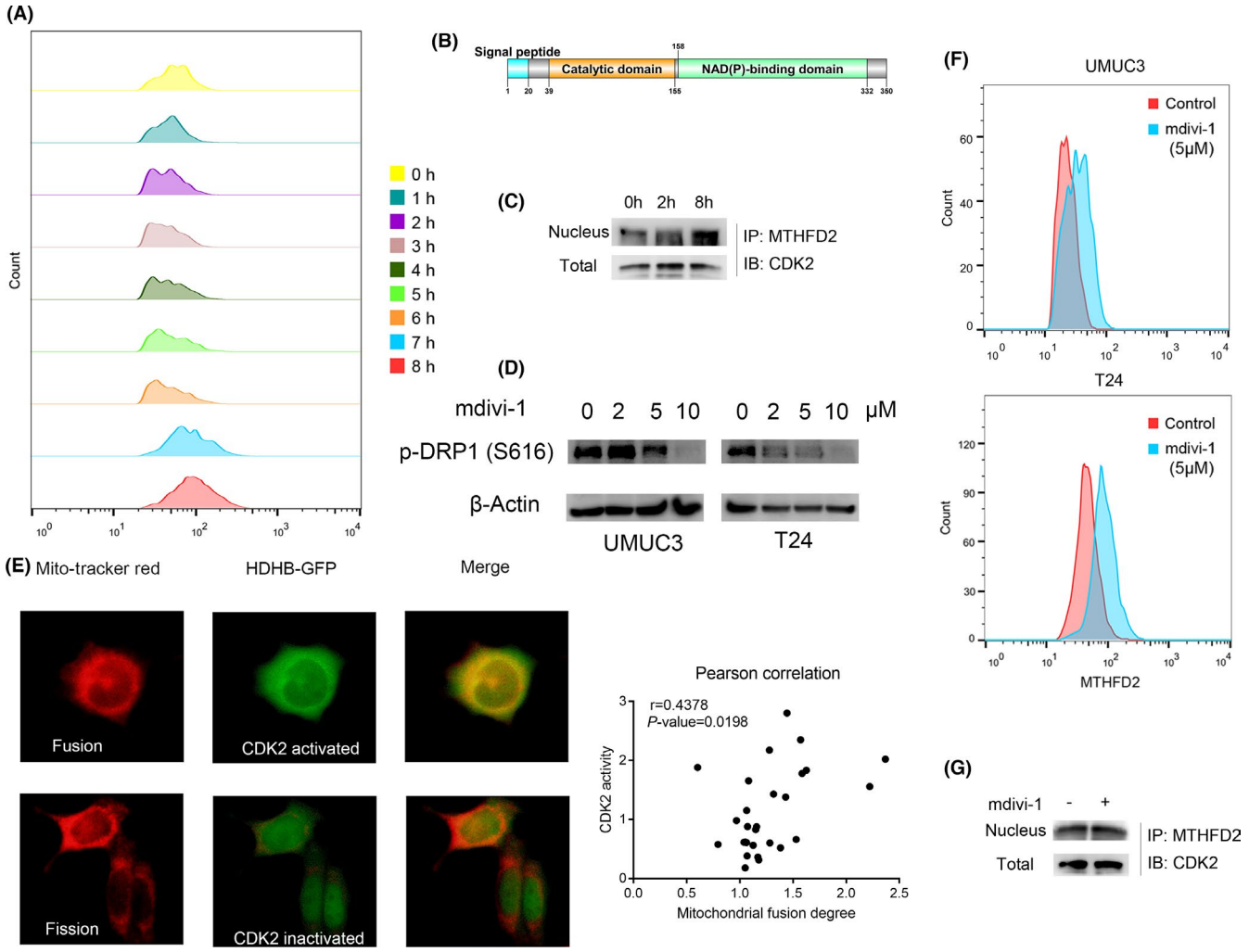

FIGURE 5 MTHFD2 translocated into the nucleus associated with mitochondrial fusion in the cell cycle. A, Nuclear expressed MTHFD2 variation released after nocodazole synchronizing in UMUC3 bladder cancer cells. B, Protein region structure of MTHFD2. C, Precipitation level between MTHFD2 and CDK2 through different cell phases in nocodazole synchronized UMUC3 bladder cancer cells. D, Efficacy of mitochondrial fusion agonist Mdivi-1 by concentration in bladder cancer cells. E, Fluorescence images for the intensity degree of mitochondria gathering around the nuclear envelope represented mitochondrial dynamics[34] and the ratio of fluorescence intensity between the nucleus and cytoplasm represented CDK2 activity,[15] and the Pearson correlation between the above fluorescence intensity ratio in 293T cells. F, Nuclear MTHFD2 expression change when treating with mitochondrial fusion agonist Mdivi-1 in bladder cancer cells by flow cytometry. G. Precipitation level change between MTHFD2 and CDK2 when treating with Mdivi-1 in the nucleus and total cell lysate of UMUC3 bladder cancer cells

acetylation of this promoter region, which limited the transcription activity of MTHFD2 (Figures 4E,F, and S3E). As E2F1 is one of the key factors that initiate cell replication, the transcriptional regulation of MTHFD2 by E2F1 allowed it to participate in the cell cycle.

3.5 | MTHFD2 translocation into nucleus associated with mitochondrial fusion in cell cycle

The protein sequence of MTHFD2 showed that it had an N-terminal mitochondrial signal peptide that permitted it to enter the mitochondria and catalyze metabolic reactions (Figure 5B). However, its mechanism regarding nuclear localization remains unclear. None of the nuclear localization sequences (NLSs) were predicted for MTHFD2, indicating that the entrance of MTHFD2 into the nucleus was probably achieved by some partner proteins. We found that the content of nuclear MTHFD2 was variable throughout the cell cycle. It elevated approximately when synchronized cells transited to the S-phase. Moreover, it had a higher probability of precipitating with CDK2 at that time (Figure 5A,C). It has been reported that the mitochondria have a dynamic morphology during the cell cycle.[25] Fluorescence images showed a correlation between CDK2 activity and the degree of mitochondrial fusion (Figure 5E). When applying a fission inhibitor that promoted mitochondrial fusion to mimic

S-phase mitochondria, MTHFD2 was found to be increased in the nucleus (Figure 5D,F). In addition, the binding between MTHFD2 and CDK2 also increased (Figure 5G). These results preliminarily showed that the translocation of MTHFD2 to the nucleus may be associated with mitochondrial morphological changes.

4 | DISCUSSION

The present study demonstrates a "moonlighting" effect of MTHFD2, which activates CDK2 in the cell cycle aside from acting as a serine metabolic enzyme. The localization of MTHFD2 is usually in the mitochondria, but we found that MTHFD2 was also distributed in the nucleus in bladder cancer cells, which presents an unexpected role. It has been reported that in some cell lines of either *Homo sapiens* or rat, MTHFD2 is expressed in the nucleus, but the function of nuclear MTHFD2 is still unclear.[13,26] The reports have commonly regarded that the nuclear MTHFD2 participates in the cell cycle. However, whether it regulates the replication process or precipitates with cdk1 to execute an unknown function in different cells remains uncertain. Similarly, we showed that MTHFD2 combines with CDK2 and bi-directionally regulates replication in the G1-S phase by activating E2F1.

The activation of CDK2 arises from the G1-S phase and remains throughout the cell cycle, serving as a multi-phase controller that regulates the cell cycle in different ways.[14] The switching on of the activity of CDK2 usually requires its phosphorylation and bonding with different cyclins.[27] We identified a combination of MTHFD2, CDK2, and Rb at an activated site on Rb phosphorylated by CDK2 and confirmed that the interaction order of the proteins was that MTHFD2 precipitated and activated CDK2 to phosphorylate Rb.

E2F1 is critical in cell replication, permitting rapid cell expansion. The accumulation of E2F1 is highly correlated with the onset of replication.[28] Our data show that overexpression of MTHFD2 activates E2F1 by releasing it from the Rb complex, which is detected by the acetylation of E2F1 and its binding to DNA as a transcription factor. E2F1 activation is a powerful sponsor for tumor cell proliferation. In conclusion, MTHFD2 activated E2F1 through the CDK2-Rb complex to support tumor cell growth.

From our analyses we found that the activation of CDK2 by MTHFD2 was similar to the way cyclins work, therefore we hypothesized that MTHFD2 would also perform like cyclins in the nucleus. Although we found no expression variation of MTHFD2 with respect to its total amount, its nuclear expression was changed in nocodazole-treated synchronized cells. We found that MTHFD2 increased in the early S phase and M phase, and the precipitation between MTHFD2 and CDK2 in the nucleus changed similarly. These results suggest that MTHFD2 enters the nucleus at nearly the S phase and lasts until the end of mitosis. In addition, MTHFD2 transcription could be regulated by E2F1 and CDK2 activity, suggesting that MTHFD2 can be expressed at a certain phase of the cell cycle.

In agreement, we have learned that mitochondria display dynamic morphological changes throughout the cell cycle, showing a hyper-fusion tubular-like form during the G1–S-phase transition.[19,29] Therefore, we wondered whether this mitochondrial fusion would contribute to the mitochondrial translocation of MTHFD2 into the nucleus. Based on our data, the levels of the nucleus-localized MTHFD2 slightly increased when promoting mitochondrial fusion. Whether it shows a physiological significance or is merely caused by an error of measurement should be discussed using further tests on the effect of mitochondrial dynamics.

The limitations of this study are as described here. First, the binding sites and the structural conformation of MTHFD2 bound to CDK2 remain unknown. It would be critical to prove whether the mitochondrially located MTHFD2 participates in the precipitation. AS an effective method to separate the non-metabolic MTHFD2 and simultaneously maintain its metabolic function in cells is lacking, most experiments focusing on the non-metabolic function of MTHFD2 are based on artificial expression or drug treatment, which may disturb the physiological function of cells. In conclusion, we found that MTHFD2 could activate CDK2 in the cell cycle aside from acting as a serine metabolic enzyme.

ACKNOWLEDGMENTS

This work was supported by the Shenyang Plan Project of Science and Technology (Grant No. F19-112-4-098), National Key R&D Plan Key Research Projects of Precision Medicine (2017YFC0908000), Shenyang Clinical Medical Research Center (Grant No. 20-204-4-42), and Liaoning Clinical Medical Research Center (Grant No. [2020]44). YJ and CK provided the funds. XL designed the experiment, performed the experiments, analyzed the data, and prepared the manuscript. SL and CP provided some ideas on study design. ZZ and XZ supervised the experimental process and edited the manuscript.

CONFLICT OF INTEREST

The authors have no conflicts of interest. The funding agency did not participate in the design of the study, collection, analysis, and interpretation of data, or in writing the manuscript.

ORCID

Xi Liu https://orcid.org/0000-0002-8700-632X

REFERENCES

1. Lawson ARJ, Abascal F, Coorens THH, et al. Extensive heterogeneity in somatic mutation and selection in the human bladder. *Science*. 2020;370:75-82.
2. Nishimura T, Nakata A, Chen X, et al. Cancer stem-like properties and gefitinib resistance are dependent on purine synthetic metabolism mediated by the mitochondrial enzyme MTHFD2. *Oncogene*. 2019;38:2464-2481.
3. Shin M, Momb J, Appling DR. Human mitochondrial MTHFD2 is a dual redox cofactor-specific methylenetetrahydrofolate dehydrogenase/methenyltetrahydrofolate cyclohydrolase. *Cancer Metab*. 2017;5:11.
4. Yang C, Zhang J, Liao M, et al. Folate-mediated one-carbon metabolism: a targeting strategy in cancer therapy. *Drug Discov Today*. 2021;26(3):817-825.

5. Ju HQ, Lu YX, Chen DL, et al. Modulation of redox homeostasis by inhibition of MTHFD2 in colorectal cancer: mechanisms and therapeutic implications. *J Natl Cancer Inst*. 2019;111:584-596.
6. Nilsson R, Jain M, Madhusudhan N, et al. Metabolic enzyme expression highlights a key role for MTHFD2 and the mitochondrial folate pathway in cancer. *Nat Commun*. 2014;5:3128.
7. Green NH, Galvan DL, Badal SS, et al. MTHFD2 links RNA methylation to metabolic reprogramming in renal cell carcinoma. *Oncogene*. 2019;38:6211-6225.
8. Ducker GS, Rabinowitz JD. One-carbon metabolism in health and disease. *Cell Metab*. 2017;25:27-42.
9. Wan X, Wang C, Huang Z, et al. Cisplatin inhibits SIRT3-deacetylation MTHFD2 to disturb cellular redox balance in colorectal cancer cell. *Cell Death Dis*. 2020;11:649.
10. Xu D, Shao F, Bian X, Meng Y, Liang T, Lu Z. The evolving landscape of noncanonical functions of metabolic enzymes in cancer and other pathologies. *Cell Metab*. 2021;33:33-50.
11. Li Y, Zhao J, Liu Z, et al. De NOVo prediction of moonlighting proteins using multimodal deep ensemble learning. *Front Genet*. 2021;12:630379.
12. Zhu Z, Leung GKK. More than a metabolic enzyme: MTHFD2 as a novel target for anticancer therapy? *Front Oncol*. 2020;10:658.
13. Yue L, Pei Y, Zhong L, et al. Mthfd2 modulates mitochondrial function and DNA repair to maintain the pluripotency of mouse stem cells. *Stem Cell Rep*. 2020;15:529-545.
14. Chao HX, Fakhreddin RI, Shimerov HK, et al. Evidence that the human cell cycle is a series of uncoupled, memoryless phases. *Mol Syst Biol*. 2019;15:e8604.
15. Spencer SL, Cappell SD, Tsai FC, Overton KW, Wang CL, Meyer T. The proliferation-quiescence decision is controlled by a bifurcation in CDK2 activity at mitotic exit. *Cell*. 2013;155:369-383.
16. van den Heuvel S, Harlow E. Distinct roles for cyclin-dependent kinases in cell cycle control. *Science*. 1993;262:2050-2054.
17. Tabara LC, Morris JL, Prudent J. The complex dance of organelles during mitochondrial division. *Trends Cell Biol*. 2021;31(4):241-253.
18. Pernas L, Scorrano L. Mito-morphosis: mitochondrial fusion, fission, and cristae remodeling as key mediators of cellular function. *Annu Rev Physiol*. 2016;78:505-531.
19. Mitra K, Wunder C, Roysam B, Lin G, Lippincott-Schwartz J. A hyperfused mitochondrial state achieved at G1-S regulates cyclin E buildup and entry into S phase. *Proc Natl Acad Sci USA*. 2009;106:11960-11965.
20. Nishitani H, Lygerou Z. Control of DNA replication licensing in a cell cycle. *Genes Cells*. 2002;7:523-534.
21. Langfelder P, Horvath S. WGCNA: an R package for weighted correlation network analysis. *BMC Bioinformatics*. 2008;9:559.
22. Yu G, Wang LG, Han Y, He QY. clusterProfiler: an R package for comparing biological themes among gene clusters. *OMICS*. 2012;16:284-287.
23. Chin CH, Chen SH, Wu HH, Ho CW, Ko MT, Lin CY. cytoHubba: identifying hub objects and sub-networks from complex interactome. *BMC Syst Biol*. 2014;8(Suppl 4):S11.
24. Leman AR, Noguchi C, Lee CY, Noguchi E. Human timeless and tipin stabilize replication forks and facilitate sister-chromatid cohesion. *J Cell Sci*. 2010;123:660-670.
25. Mitra K. Mitochondrial fission-fusion as an emerging key regulator of cell proliferation and differentiation. *BioEssays*. 2013;35:955-964.
26. Gustafsson Sheppard N, Jarl L, Mahadessian D, et al. The folate-coupled enzyme MTHFD2 is a nuclear protein and promotes cell proliferation. *Sci Rep*. 2015;5:15029.
27. Li Y, Zhang J, Gao W, et al. Insights on structural characteristics and ligand binding mechanisms of CDK2. *Int J Mol Sci*. 2015;16:9314-9340.
28. Matson JP, House AM, Grant GD, Wu H, Perez J, Cook JG. Intrinsic checkpoint deficiency during cell cycle re-entry from quiescence. *J Cell Biol*. 2019;218:2169-2184.
29. Tian T, Lv X, Pan G, et al. Long noncoding RNA MPRL promotes mitochondrial fission and cisplatin chemosensitivity via disruption of Pre-miRNA processing. *Clin Cancer Res*. 2019;25:3673-3688.

SUPPORTING INFORMATION

Additional supporting information may be found in the online version of the article at the publisher's website.

How to cite this article: Liu X, Liu S, Piao C, et al. Non-metabolic function of MTHFD2 activates CDK2 in bladder cancer. *Cancer Sci*. 2021;112:4909–4919. https://doi.org/10.1111/cas.15159